Evaluation of field concrete deterioration under real conditions of seawater attack

Ahmed Mahmoud Ragab [a], Mohamed Adel Elgammal [b], Osama AbdelGhafour Hodhod [a], Tamer ElSayed Ahmed [b,*]

[a] Structural Engineering Department, Cairo University, Egypt
[b] Engineering Division, National Research Center of Egypt, Egypt

HIGHLIGHTS

- Study the seawater attack on concrete specimens from the wave's repellent blocks.
- Trace the interaction of concrete with chlorides and sulfates in seawater.
- The specimens tested with XRF, SEM, EDX, and water soluble chloride test.
- SEM and EDX analyses prove that siliceous aggregate particles act as inert material.
- Mapping Technique determines the locations of cracks, voids, and capillary pipes.

ARTICLE INFO

ABSTRACT

In order to study the long term behavior of concrete structures under the natural exposure to aggressive seawater attack, concrete samples are taken from the wave's repellent blocks at seashore in the north coast of the Mediterranean Sea. The samples cover a wide range of various exposure times differ from 4 years to more than 60 years. The samples composed from diverse concrete constituents and obtained from different locations along the seashore. The tests (XRF, SEM, EDX, water soluble chloride content using photometer techniques) where conducted on the extracted concretes.

© 2016 Elsevier Ltd. All rights reserved.

1. Introduction

The chemical action of seawater on concrete is mainly due to the presence of $MgSO_4$, $MgCl_2$ with NaCl, as well as other dissolved salts [1].

The interaction of concrete with chlorides and sulfates in seawater leads to modification of the intrinsic concrete properties. Seawater contains high concentration of chlorides relative to less concentration of sulfates. Since, the concentration of ions in typical seawater is almost around 19,090 ppm of Chloride, and 2233 ppm sulfate. The chemical analysis show that the chloride concentration increases up to ten times sulfate concentration in typical seawater [2].

The ingress of sulfates constitutes a major risk of chemical aggression for concrete causing destructive expansion, and loss of bond between the cement paste and aggregate leads to strength loss [3]. These processes are commonly caused as a result of reactions between the tricalcium aluminate (C3A) in the Portland cement and sulfate ions to form expansive ettringite compound [4].

However, the high chloride concentration of the seawater solution could reduce the expansive nature of the ettringite formed by sulfate attack. So, chlorides have a tendency to bind C3A in the cement to produce chloroaluminate compounds, such as Friedel's salt, which do not cause any expansion. Also, ettringite formation

Table 1
Sample location and its corresponding chloride and sulfate ions concentrations.

Name	Location	Start of exposure (Year)	Geographic location		Ions concentrations of seawater (ppm)	
			North	East	Chloride	Sulfate
T08	El-Tarh	2008	31° 16′ 17″	30° 07′ 45″	21,200	2101
M07	El-Mansheia	2007	31° 12′ 03″	29° 53′ 30″	19,400	2155
T03	El-Tarh	2003	31° 16′ 17″	30° 07′ 40″	21,200	2101
Q87	El-Qalaa	1987	31° 12′ 48″	29° 53′ 11″	19,400	2155
T85	El-Tarh	1985	31° 16′ 17″	30° 07′ 50″	21,200	2101
Q50	El-Qalaa	1950	31° 12′ 49″	29° 53′ 10″	19,400	2155

Table 2
Concrete ingredients and its corresponding compressive strength.

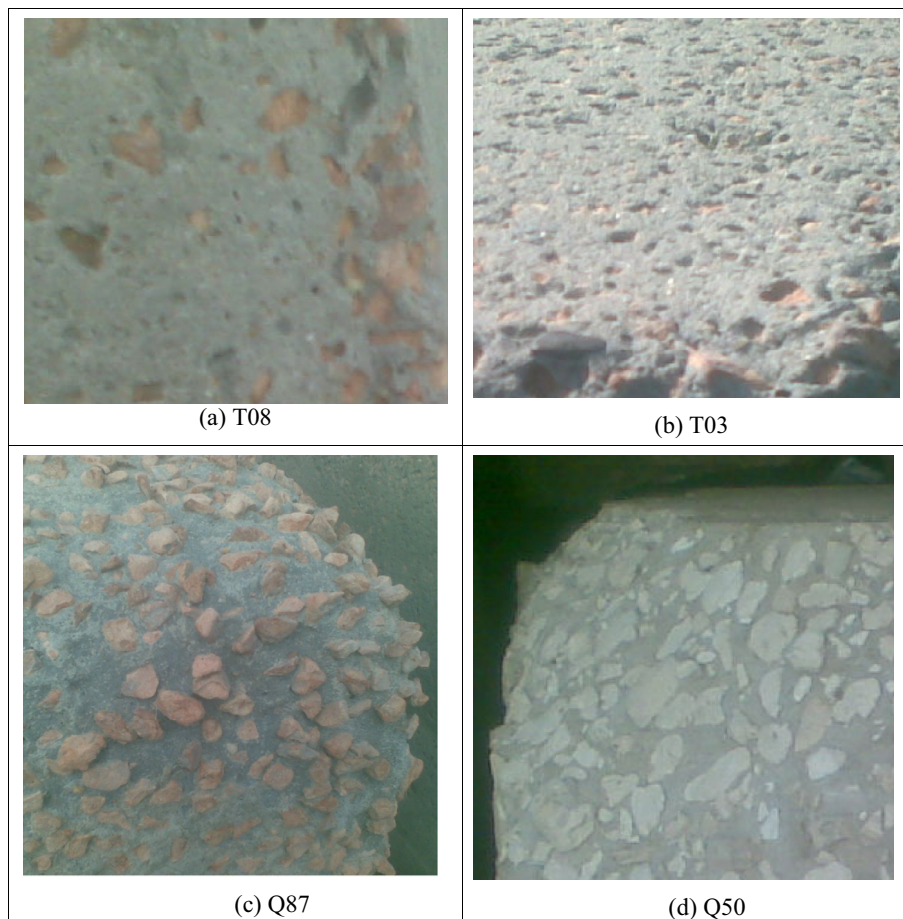| Name	W/C	Water (kg/m^3)	Cement (kg/m^3)	Fine aggregate (kg/m^3)	Coarse aggregate (kg/m^3)	Admixture (Liter/m^3)	Compressive strength (kg/cm^2)
T08	0.34	135	400 (SRC)	684	1164 Dolomite	4 Sikament MG	371
M07	0.33	133	400 (SRC)	692	1180 Dolomite	4.5 Sikament MG	431
T03	0.34	135	400 (SRC)	684	1164 Dolomite	4 Sikament MG	350
Q87	0.47	165	350 (SRC)	630	1260 Dolomite	1 MC Admix.	312
T85	0.47	165	350 (SRC)	630	1260 Gravel	1 MC Admix.	300
Q50	0.65	196	300 (SRC)	598	1195 Lime stone	0	225

in chloride-rich environments is not associated with expansion and cracking [5].

The ingress of chloride into concrete causes fast and severe corrosion of the steel reinforcement. This reduces the cross-section of the reinforcement and consequently leads to the loss of its load carrying capacity [6].

The alkalinity medium of concrete prevents the reinforcement corrosion process until the chloride content at the steel surface has reached a certain threshold value. This value is often stated as critical chloride content or chloride threshold value [7]. So, the determination of chloride content within concrete indicates to how far the deterioration of the concrete is.

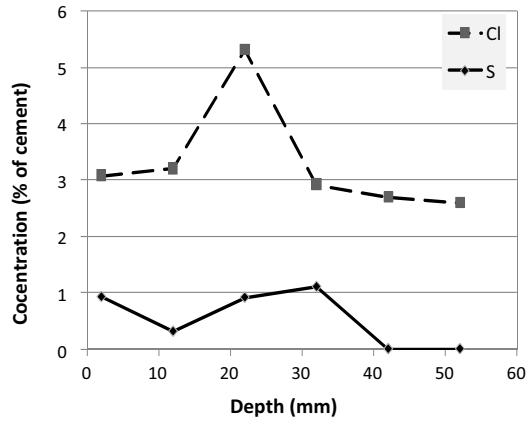(a) T08

(b) T03

(c) Q87

(d) Q50

Fig. 1. Images of concrete blocks exposed to seawater attack.

Table 3
Concrete erosion depth and carbonation depth for all specimens.

| Name	T08	M07	T03	Q87	T85	Q50
Concrete erosion (mm)	2	1	3	10	15	50
Carbonation (mm)	4	2	6	15	18	23

However, the majority of the studies have been conducted on laboratory samples like cement paste, mortar or concrete produced and exposed to artificial seawater in a laboratory environment with different chloride and sulfate concentrations [8–11].

There are relatively few case studies that provide detailed information about the micro-structural and chemical changes taking place in field concrete during seawater or ground water attack. These studies generally were carried out with a view toward recording the common deterioration signs of existing old concrete structures taking into account the long term behavior of concrete structures after long time of exposure to aggressive media. These researches present significant results under real conditions of full scale specimens exposed to natural climatic weather and continuous attack [12–14].
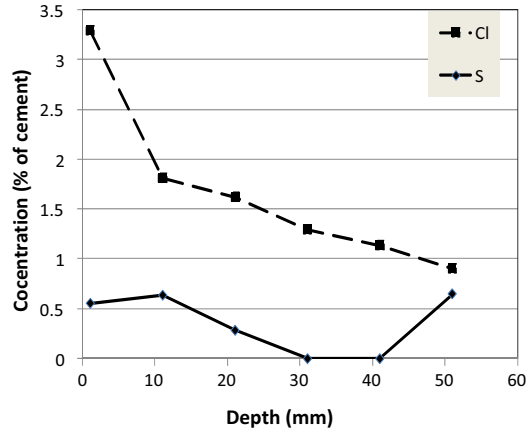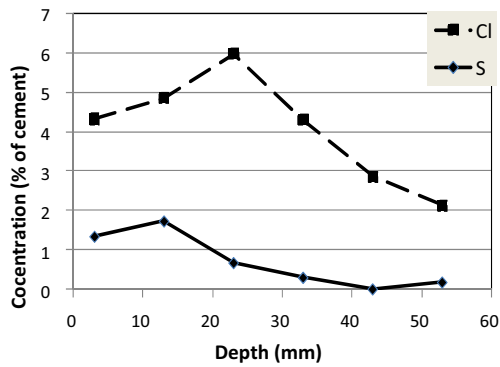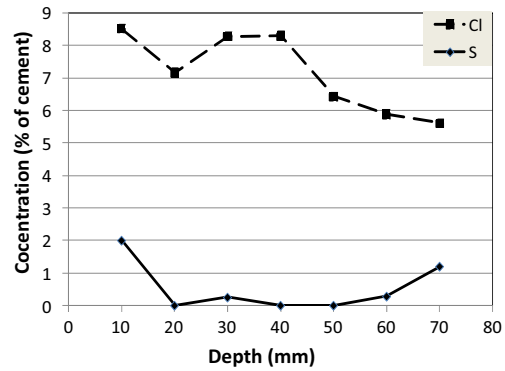

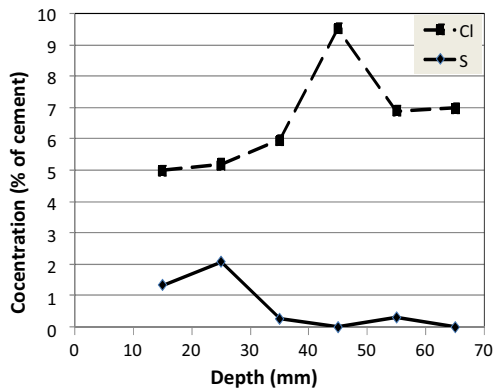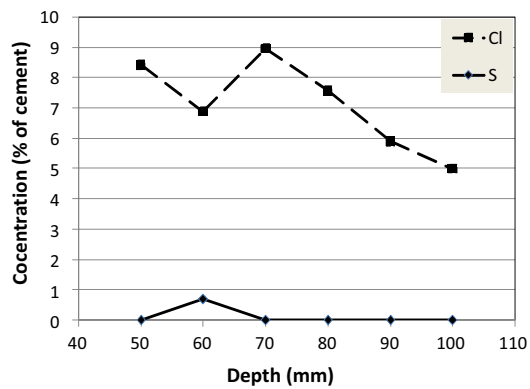Fig. 2. Total chloride and sulfate ions concentrations in the concrete specimens along with concrete depths of exposure to seawater.

As an instance, samples collecting from existing docks structures after twenty-seven years of seawater exposure in Portugal built with a poor-quality concrete was studied. The higher deterioration rates were observed in zones where the concrete surface is subjected to wetting and drying cycles of seawater. In these very aggressive exposure conditions, reinforcement corrosion rates in excess of 500 μm/year were measured [15].

The objective of this study is to investigate the effect of seawater on the properties of hardened concrete durability. An experimental program is designed and performed to discover the way to achieve the optimum concrete mixture with chemical ingredients that has required compressive strength at certain level of durability.

2. Experimental work

2.1. Material

The examined specimens were taken from the corner edge of the wave's repellent blocks at seashore in the tidal zone where the specimens on beach were sprinkled periodically with seawater. Samples taken from six different locations along the north coast associated with different chlorides and sulfates ions concentrations. The exposure durations of the samples differ from 4 years to more than 60 years as presented in Table 1. Note that the extracted ions concentrations are at the experimental work.

The wave's repellent blocks were constructed under governmental technical supervision of the Seashore Protection Association (SPA) [16] which follows the minister of irrigation in Egypt.

The Seashore Protection Association (SPA) having all the gathered data presented in Table 2 regarding the diverse concrete constituents of each block associated with the corresponding compressive strength. All mixes used sulfate-resisting cement (SRC) with various amounts. Obvious observations of concrete deteriorations across years tend to increase the cement content in the recently constructed blocks. Different types of coarse aggregate are used according to the source availability near sites. Water reducer admixtures are added to decrease water to cement ratio (W/C) and also decrease permeability and consequently enhance mechanical properties associated with more durable concrete. Measured compressive strength recorded on cylinder of dimensions 15 cm diameter and 30 cm depth.

2.2. Methodology

The specimens were taken from the corner edge of the wave's repellent blocks at seashore in the tidal zone. Then, the depth of carbonation is measured by spray phenolphthalein indicator onto the surface of a freshly split concrete sample. The solution is a colorless base indicator, which turns purple when the pH is above 9.0 [17].

The specimens were sliced using a diamond wheel saw. Segments approximately 1 cm thick were taken across the length of the core. Each segment was about 6 cm in length and about 6 cm in width. Each slice was broken to pieces of 1 cm³ which represent the examined concrete sample at every depth.

The 1 cm³ pieces were gold coated prior to examination under the Scanning Electron Microscopy (SEM) combined with Energy-dispersive X-ray (EDX) analysis. The EDX analysis gives the full element composition of the concrete sample including the total chloride content. The total chloride content contains free chloride and bound chloride. The same analysis determines the sulfate content. A comparative study was conducted with X-ray Fluorescence Analysis (XRF) for two specimens to give full chemical analysis of well grounded concrete.

In order to determine the free chloride content which is responsible for steel corrosion leaching technique is used. Ground samples are put in distilled water as solvent and leached out the water soluble chloride. Photometer measurement system is used to quantify the amount of water soluble chloride in the specimen [18].

3. Results and discussions

Concrete structures existed at the seashore is exposed to running waves which consequently abrade its surface which is softened due to the chemical reactions. An images of deteriorated samples is shown in Fig. 1.

The erosion starts from aggregate-cement paste interfacial transition zone as a weak point and then propagates around the coarse aggregate which in turn protruded from concrete block. So, the erosion depth presented in Table 3 is the average eroded depths around the coarse aggregate.

In case of white limestone coarse aggregate, the behavior is different. So, the limestone aggregate is synchronically eroded with cement paste as shown in Fig. 1(d).

The carbonation depth measured from the remaining surface after concrete erosion as presented in Table 3. Carbonation depth increases as concrete quality decreases. Hence, higher concrete grade leads to a reduction in carbonation depth over a specific period of time [19].

According to EDX analysis, total chloride profiles of the concrete specimens associated with sulfate ion concentrations for different concretes at varying exposure time (4, 5, 9, 25, 27, and 62 years) are presented in Fig. 2.

Fig. 2 illustrates that the chloride concentration at the concrete surface is almost same as the chloride concentration in seawater and then the chloride concentration is increased due to the accumulation of chloride ions forming chloroaluminate compounds which in turn block the pores and prevent more access of chloride or sulfate into concrete

Fewer amounts of sulfates measured in the specimens is due to sulfate resisting cement used which is made with no or low gypsum ($CaSO_3$) added to the clinker. The high Cl concentration of seawater could play an important role by binding the C3A to form chloroaluminate compounds, such as Friedel's salt and also by lowering the expansive potential of ettringite. So, it has afforded better protection against ingress of the sulfate ions into concrete [2].

Chloride content within millimeters at the concrete surface is anomalously fewer. It may also be due to the concrete skin which

Table 4
Quantitative analyses XRF (Q87).

Main constituents	(Weight %) of mortar At depth = 10 mm	(Weight %) of mortar At depth = 70 mm
SiO_2	66.94	67.57
TiO_2	0.12	0.15
Al_2O_3	1.26	1.25
Fe_2O_3	1.07	1.13
ZrO_2	0.03	0.03
MnO	0.05	0.00
MgO	0.70	0.59
CaO	12.75	14.81
Na_2O	1.73	1.33
K_2O	0.35	0.31
SrO	0.11	0.15
P_2O_5	0.05	0.03
SO_3	0.95	0.73
Rb_2O	0.02	0.02
Br	0.01	0.00
Cl	2.67	1.74
L.O.I	11.17	10.17

has a different composition, compare to the internal concrete. A contact with the moulds, segregation of aggregates or dielectric reaction between the concrete surface and chloride environment are attributed to a fall in the surface chloride [20,21].

Different behavior in M07 specimen with the highest chloride content at the concrete surface is measured. This is mainly due to the highest compressive strength with dense impermeable concrete and less carbonation depth recorded in this specimen. So, the total chloride concentrated at the concrete surface and decreased with depth.

Table 4 shows a sample XRF analysis compatible with EDX for the Q87. The XRF analysis is made for grounded mortar around the coarse aggregate while the EDX analysis is a chemical surface analysis. The XRF results ensure the decreasing of external elements through the depth of concrete. These XRF analysis is used to confirm the results form EDX analysis.

The water soluble chloride is responsible about steel corrosion. The monitoring of chloride content inside concrete is a key factor to specify the service life time of any structure facing harmful salty conditions. the results of water soluble chloride illustrated in Fig. 3 is convenient with the fact that increased binding capacity of cement matrix allows more free chlorides to accumulate on the surface of concrete [22]. So, the maximum chloride content exists at the concrete surface. The exposure duration to seawater scale out the amount of chlorides. Higher compressive strength and more cement content with low W/C ratio obstruct chloride ions from ingress into concrete due to concrete densification with less and discrete pores.
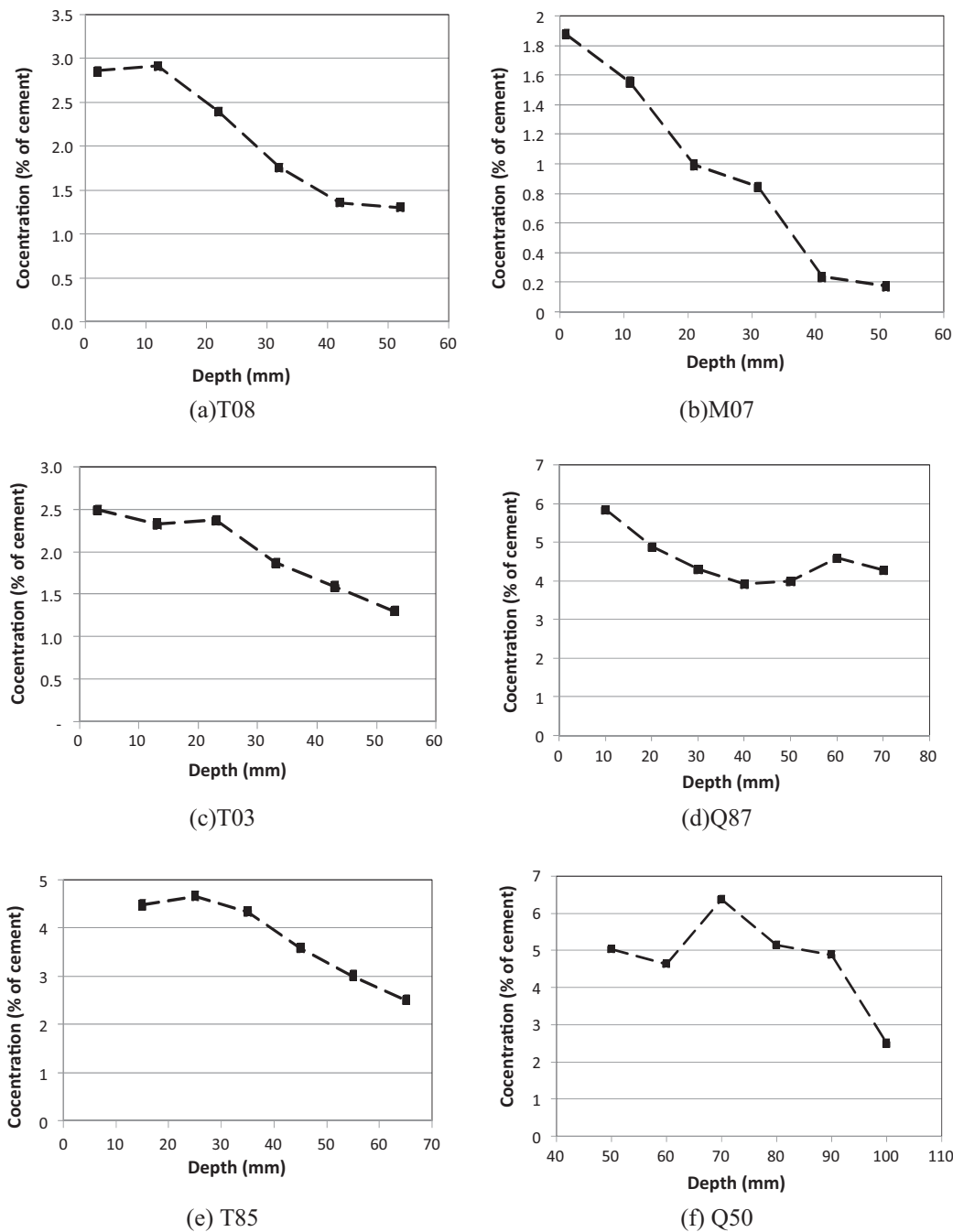

Fig. 3. Free (water soluble) chloride ions concentrations in the concrete specimens along with concrete depths of exposure to seawater.
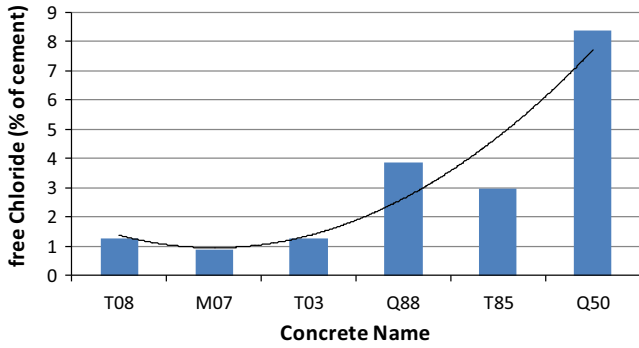
Fig. 4. Free chloride content at depth of 50 mm.

Fig. 4 illustrates the free chloride content which is the active chloride that affects the steel corrosion at the most used concrete cover at 5 cm for all concrete samples. So, by comparing the free chloride content with those allowed in the international codes of concrete we can specify the service life of structures facing the sea-water attack after long time.

3.1. Microstructural study

The scanning electron microscopy (SEM) is conducted with the aim of observing the deterioration of six different concretes exposed to seawater at different exposure periods. The study focuses on the observed features in different concrete mixes such as voids, capillary pipes, aggregate/paste transition zone, portlandite CH [$Ca(OH)_2$], Calcium Silicate Hydrate CSH [$3CaO \cdot 2SiO_2 \cdot 3H_2O$], silica gel [$SiO_2 \cdot xH_2O$], gypsum [$CaSO_4 \cdot 2H_2O$], ettringite [$3CaO \cdot Al_2O_3 \cdot 3CaSO_4 \cdot 32H_2O$], thaumasite [$CaSiO_3 \cdot CaSO_4 \cdot CaCO_3 \cdot 15H_2O$], brucite [$Mg(OH)_2$], M–S–H [$3MgO \cdot 2SiO_2 \cdot 2H_2O$], Friedel's salt [$Ca_4Al_2Cl_2(OH)_{12} \cdot 4H_2O$], Dolomite [$CaMg(CO_3)_2$], Quartz [$SiO_2$], Potassium feldspar [$KAlSi_3O_8$], or unhydrated clinker components which contain Alite C_3S [$3CaO \cdot SiO_2$], Belite C_2S [$2CaO \cdot SiO_2$], Ferrite C_4AF [$4CaO \cdot Al_2O_3 \cdot Fe_2O_3$], Aluminate C_3A [$3CaO \cdot Al_2O_3$] and any other components.

3.2. Rules of the inspection of the SEM images

In order to interpret the SEM snapshots, a survey in the previous work done in the same field of interest. Sahu et al. [23] rearrange these previously mentioned components according to relative,
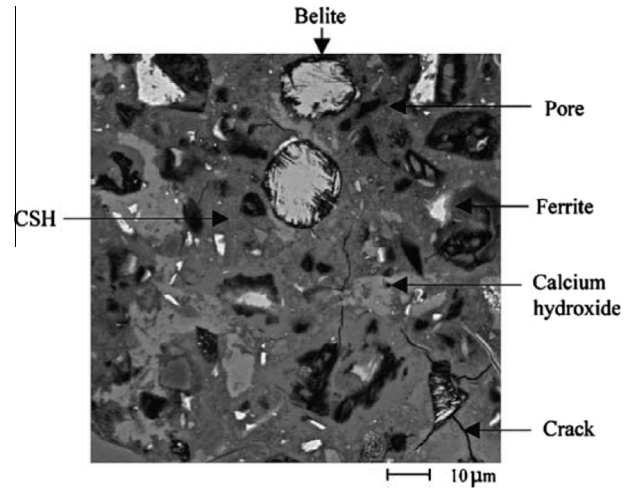

Fig. 5. Concrete components in SEM images according to grey scale.

measured image intensity as shown in Fig. 5 where, backscattered electrons are controlled by the atomic number of the material irradiated. For low atomic number materials, little scattering takes place near the surface and most of the incident electrons are absorbed within the specimen. Materials with a higher atomic number generate much more scattering at the specimen surface and consequently a greater proportion of backscattered electrons are produced. Therefore, in a backscatter electron SEM image brighter regions represent phases of higher atomic number and darker regions represent phases of lower atomic number.

Two morphological forms of calcium hydroxide are common, elongated crystals and massive shape. The elongated crystals are cross section of the hexagonal pates. These exhibit characteristics cleavage parting along basal planes and may represent early formed CH where relatively unrestricted growth allowed the formation of the ideal hexagonal habit. The term massive CH (without form) may be used where the fine grained habit shows no crystal form. This material fills voids in the CSH, and so, is probably a later occurring product of the hydration process [24]. The morphology of the majority of cement hydration C-S-H gel products is mostly cotton-shaped [25].

A selection of the backscattered electron images is given in Fig. 6. In this selection distinction between the main elements
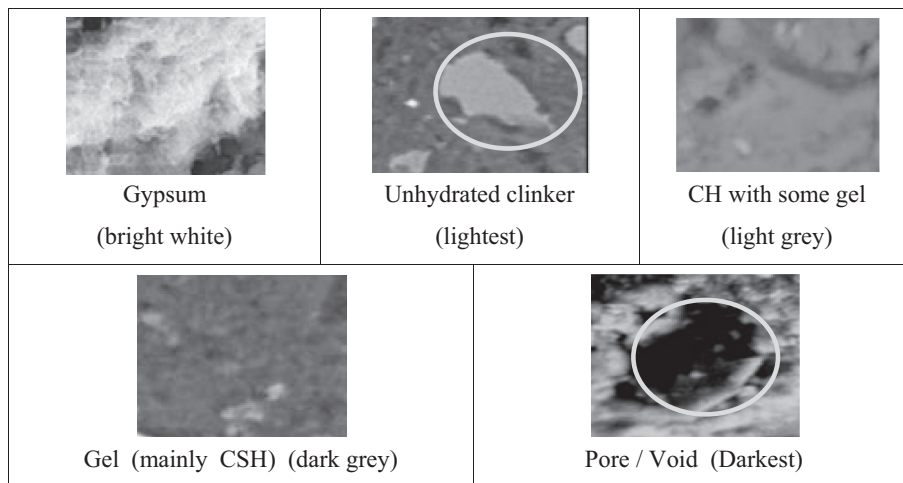

Fig. 6. Interpretation of SEM images according to grey scale.

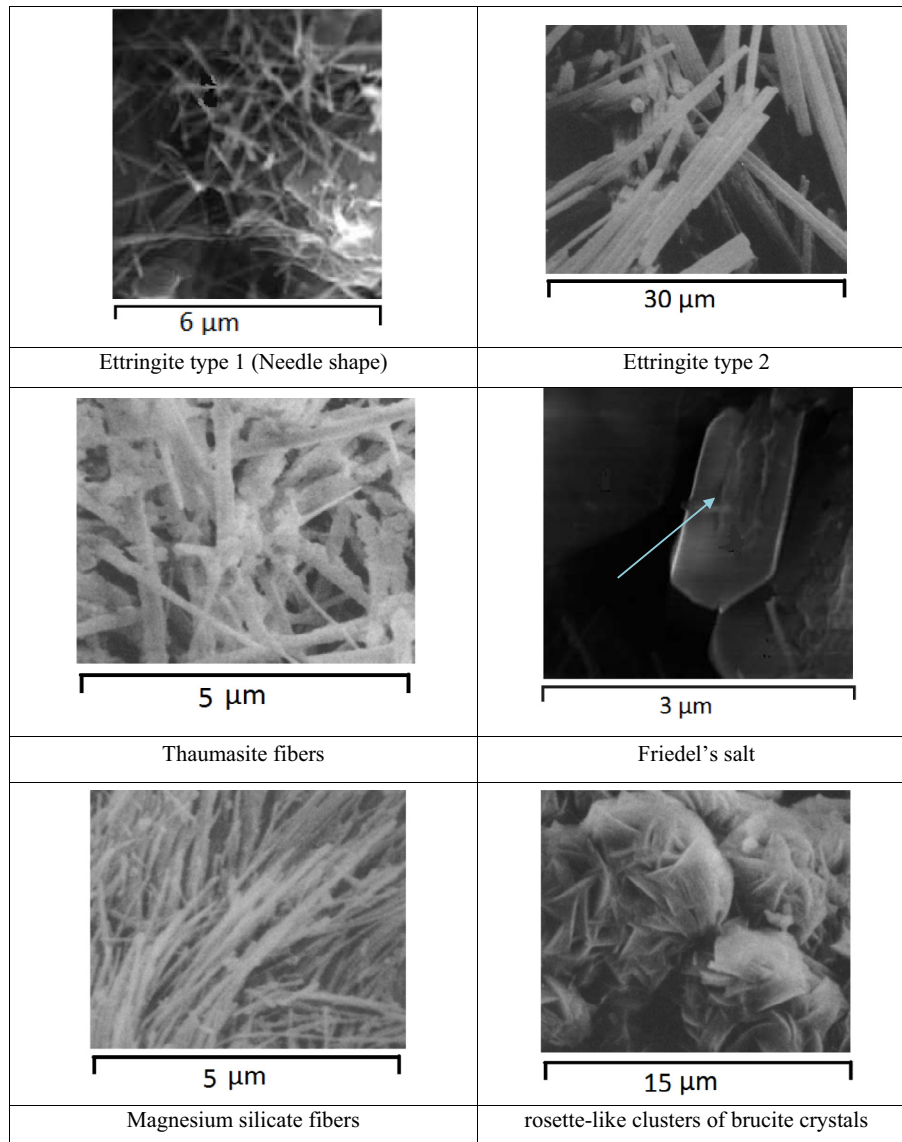| Ettringite type 1 (Needle shape) | Ettringite type 2 |
| Thaumasite fibers | Friedel's salt |
| Magnesium silicate fibers | rosette-like clusters of brucite crystals |

Fig. 7. SEM snapshots of the main compounds found in concrete exposed to seawater attack.

according to grey scale is used. The phases of interest, graded in terms of their brightness, are gypsum .lightest. > unhydrated cement grains (clinker) > calcium hydroxide .CH. > gel (predominantly calcium silicate hydrate(C-S-H)) > aluminate-bearing hydrates > aggregate > porosity and voids(darkest) [26].

SEM snapshots shown in Fig. 7 demonstrate the main compounds in concrete exposed to seawater attack. SEM shows that ettringite crystals have perfect needle-shape with hexagonal cross-section. These crystals are formed in cracks. These crystals resemble each other and tend to grow together in the same

direction. Some of the crystals are twinned and they continue to grow separately. Gypsum crystals and ettringite crystals are easily distinguished. Gypsum crystals have plate form like a mass of successive layers of ice, or fish scales. Meanwhile, ettringite crystals are needle-shaped.

While ettringite appears in two modes, The first one is long lath-like crystals which range from 10 to 100 μm and several μm thick, formed at low hydroxyl ion concentrations (i.e. with low pH values in the pore solution). In the case of hydrated cements containing significant amounts of these ettringite crystals, these

lead to high strengths and non-expansion. The second type of ettringite is rod-like crystals which range only from 1 to 2 μm long and 0.1 to 0.2 μm thick, which are formed at high hydroxyl ion concentrations. These are present during the hydration of Portland cements which at large quantities can cause expansion effects through water adsorption [27].

The morphology of Friedel's salt is hexagonal slice and its size is between 2 and 3 μm. The hydrated products of C3A are also hexagonal, but its size is no more than 1 μm and is much smaller than that of Friedel's salt while the photo for $Ca(OH)_2$ may also be hexagonal with much larger size [28].

The magnesium existed in seawater replaces the calcium in CH to form brucite $Mg(OH)_2$. The brucite forms small rosette shaped crystals in the early stages of attack. While the Magnesium silicate morphology having fibers shape. Thaumasite morphology is tangled needle shape fibers and its size is between 5 μm [29].

With the purpose of interpret the EDX analysis of this thesis, a survey in the previous work done in the same field of interest. Fig. 8 synopses the most existing compounds found in deteriorated concrete [30]. It illustrates the main elements with trace elements of gypsum, thaumasite, and ettringite compounds.

From Fig. 9 to Fig. 14, the resulted microstructures Regarding the SEM micrographs of the examined concrete is shownFig. 9 illustrates the reaction product of chloride with the calcium sulphoaluminate phases and any remaining calcium aluminates to form calcium chloroaluminate "Friedel's salt" which crystallizes as hexagonal plates. The EDX spectrum showed the presence of a significant amount of iron and silica.

Mapping in Fig. 10 illustrates clearly a siliceous sand particle with silicon element surrounded by cement matrix. The mapped location of chloride ions is almost in the cement matrix rather than sand particle.Fig. 11 is taken from a small natural siliceous sand particle. The corresponding EDX analysis demonstrates that major element is silicon and almost no chlorides and sulfates ions despite of its vicinity to concrete surface faced aggressive seawater attack.

Fig. 12 is snap on brightest location in the picture which is due to presence of gypsum compound.

Fig. 13 confirms the abundance of needle shaped ettringite incorporating limestone calcite filler. Ettringite is frequently intermixed with other sulfate-bearing phases that is exactly shown in the lightest spots confirmed the presence of gypsum compounds. There is no thaumasite investigated due to the absence of required carbonFig. 14 is taken from a natural particle which is limestone. The corresponding EDX analysis demonstrates that major element is calcium and there are a few amounts of chloride ions penetrating the limestone but it is still less than the amount of chloride ions at the surrounding cement paste.

The SEM images from Fig. 9 to Fig. 14 explain the peak of total chloride ions concentration appeared in Fig. 2 because of chloroaluminate compounds shown in the figures and confirmed by EDX analysis.
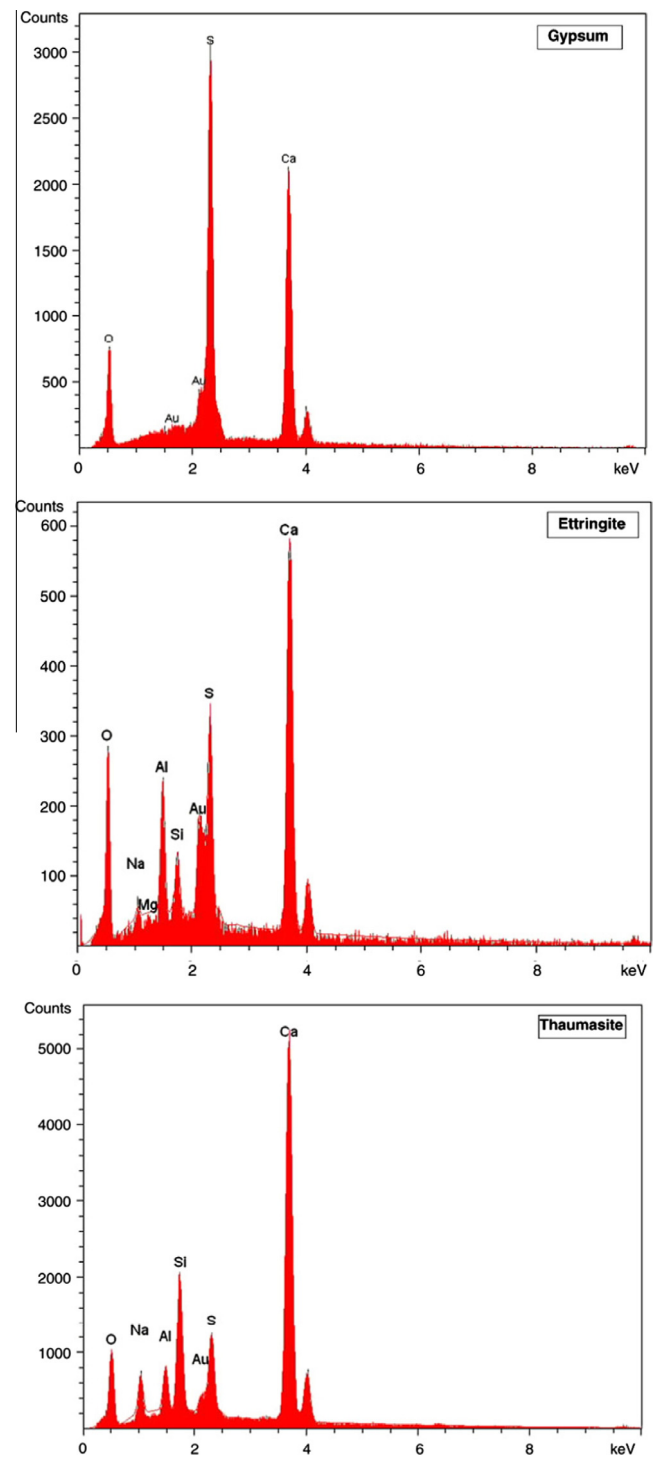
Fig. 8. EDX analysis of the main compounds found in concrete exposed to seawater attack.

Element	O K	Na K	Mg K	Al K	Si K	S K	Cl K	K K	Ca K	Fe K	Rb K	Sr K	I L	Totals
Weight%	44.82	0.15	0.61	1.99	8.17	0.91	3.96	0.07	34.2	3.65	0.52	0.3	0.67	100
Atomic%	65.57	0.15	0.59	1.72	6.81	0.66	2.61	0.04	20.0	1.53	0.14	0.08	0.12	
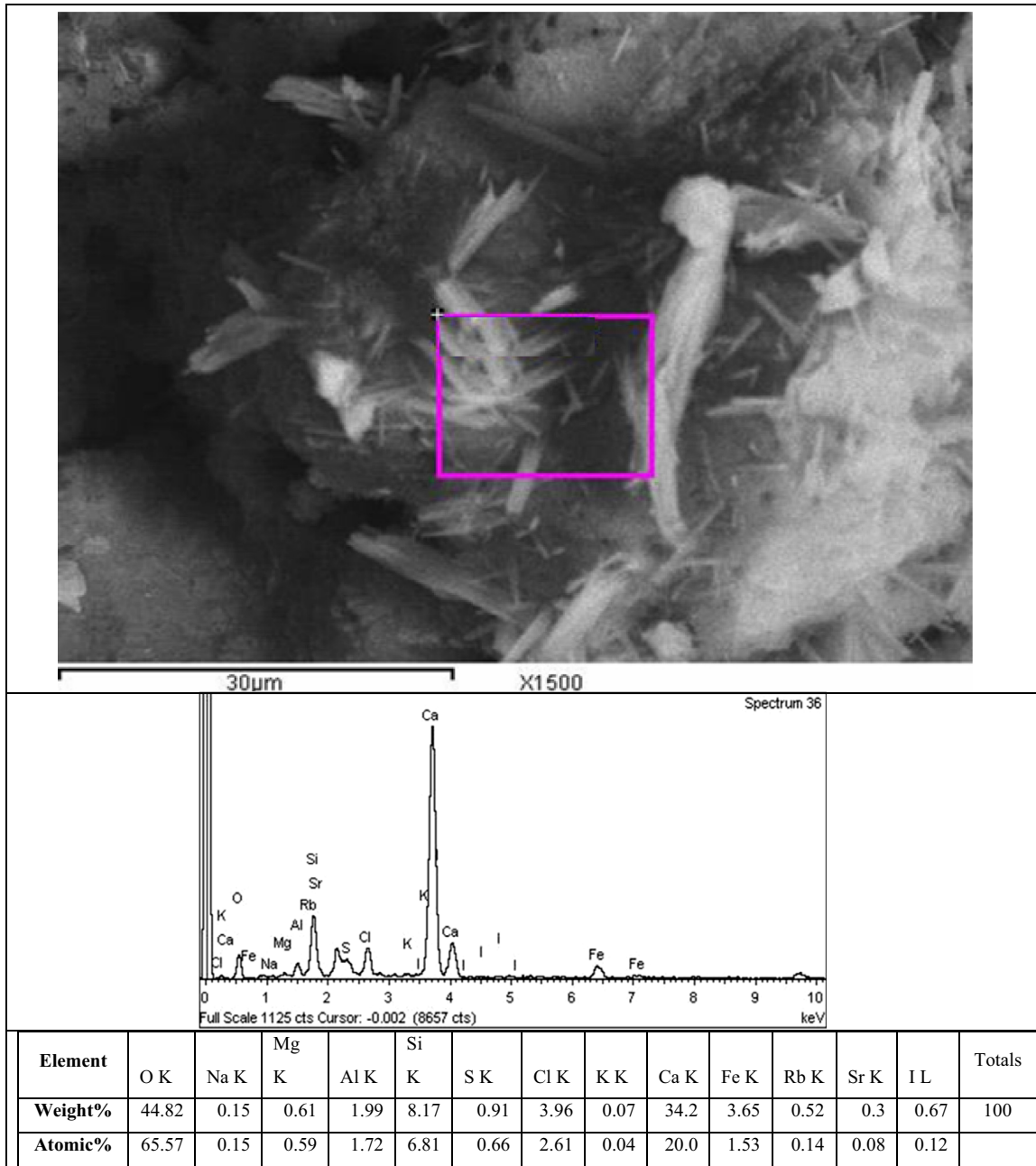
Fig. 9. SEM and its corresponding EDX analysis for T08 at depth 32 mm.

4. Conclusions

This paper study the experimental issues of the synergistic effects of sulfates and chlorides on the long term behavior of filed concrete exposed to seawater attack at the splash zone. The following major conclusions are drawn:

• Complicated nature of reactions of various concrete compounds with the chlorides, sulfates, and magnesium attack existed in seawater can result in the formation of different reaction products at different stages resulting in changes in concrete properties.

Element	C K	O K	Na K	Mg K	Si K	Cl K	K K	Ca K	Rb K	Sr K	Totals
Weight%	21.17	49.02	0.12	0.86	10.38	0.06	0.13	18.12	0.04	0.11	100
Atomic%	30.95	53.8	0.09	0.62	6.49	0.03	0.06	7.94	0.01	0.02	
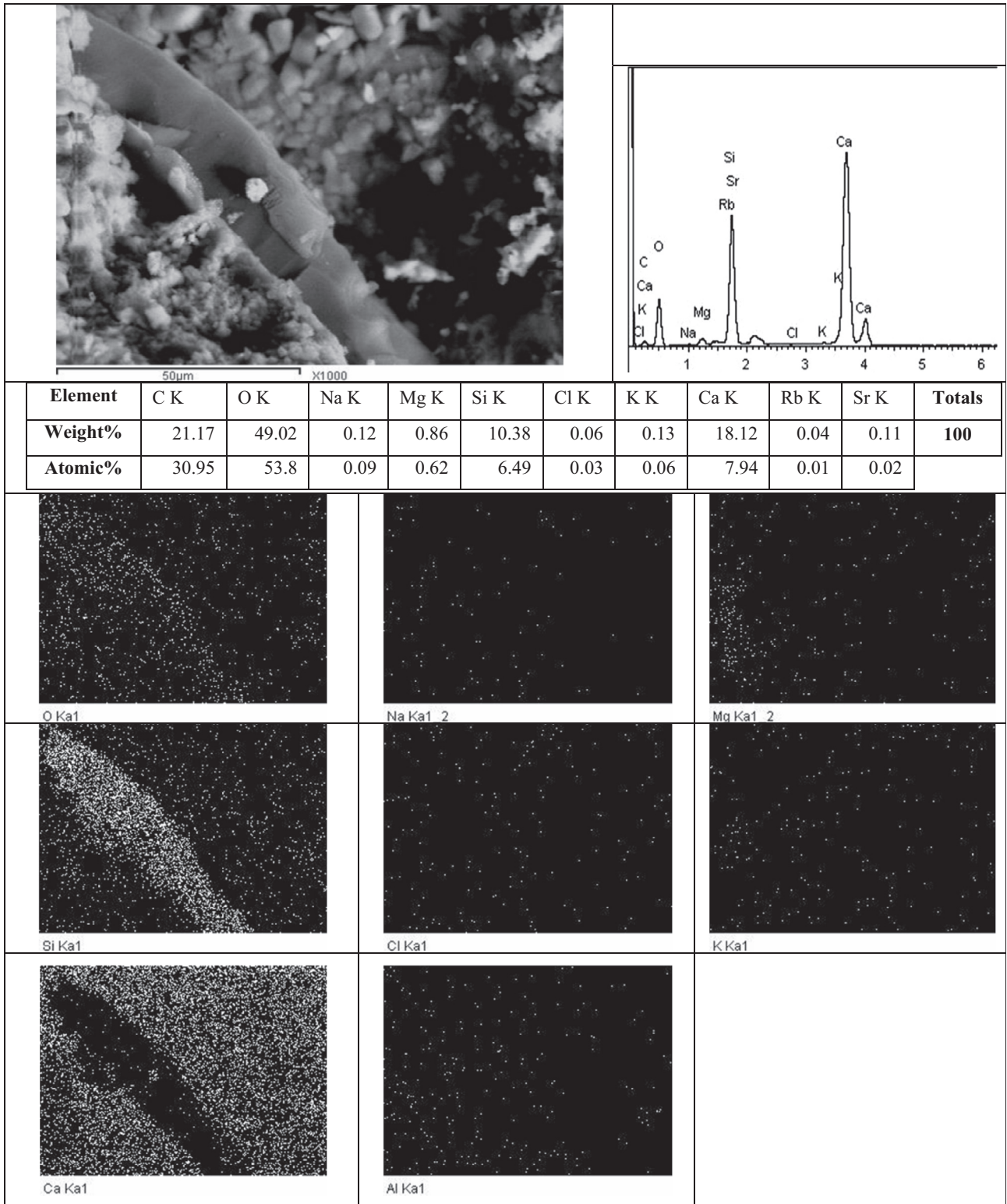
Fig. 10. SEM and its corresponding EDX analysis and mapping for M07 at depth 51 mm.

Element	C K	O K	Si K	S K	Cl K	Ca K	Totals
Weight%	3.85	54.8	40.27	-0.09	0.07	1.11	100
Atomic%	6.15	65.79	27.54	-0.05	0.04	0.53	
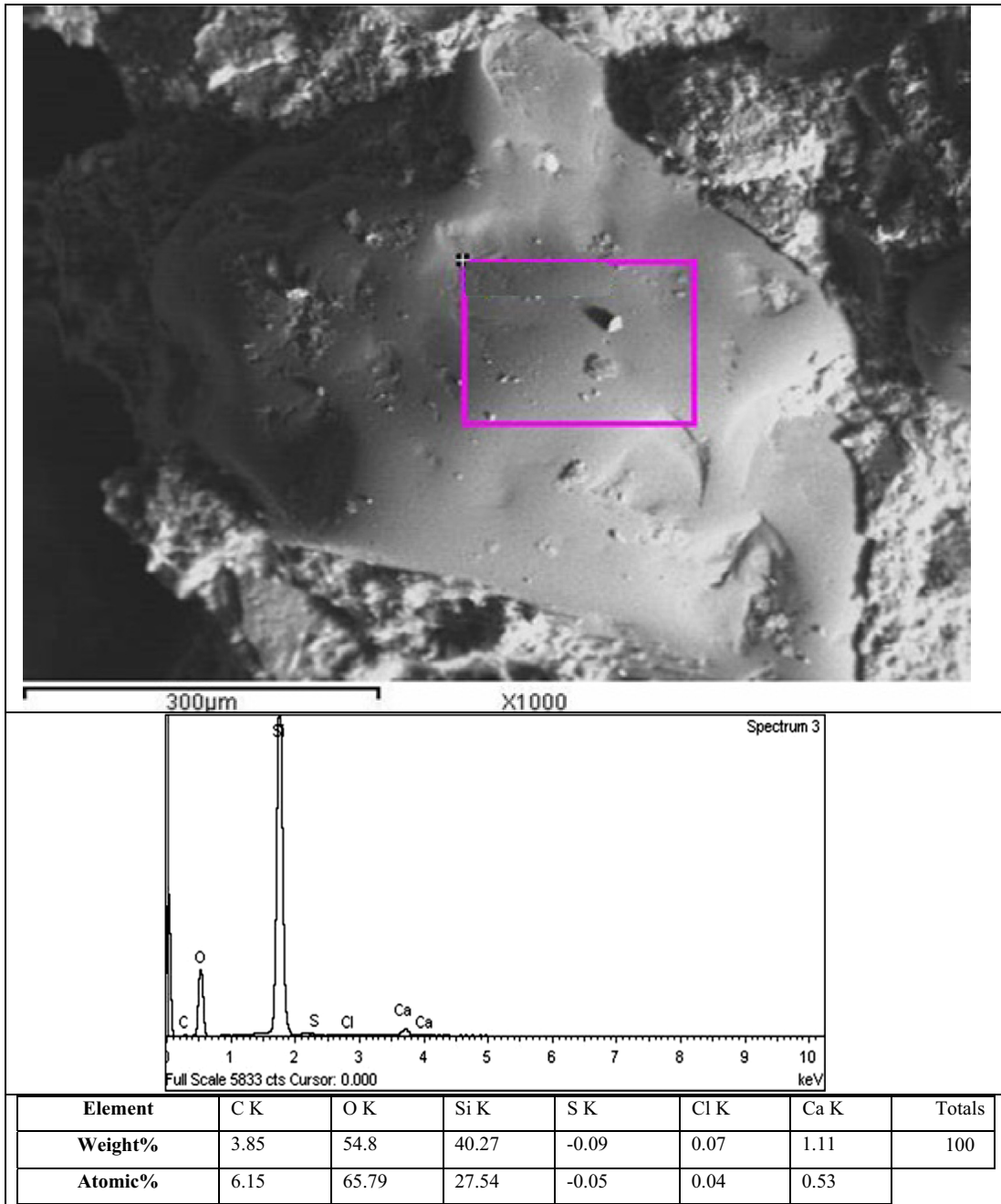
Fig. 11. SEM and its corresponding EDX analysis for T03 at depth 3 mm.

- The present study shows that the deterioration of concrete due to seawater attack progresses inwards from the exposure surface with the duration of exposure.
- The test result shows that the main deterioration processes as follows:

o Partial decomposition of CSH gel to MSH gel.
o Formation of gypsum, ettringite, and thaumasite due to the sulfate ion attack.
o Binding C_3A to form chloroaluminate compounds Friedel's salt during chloride attack.

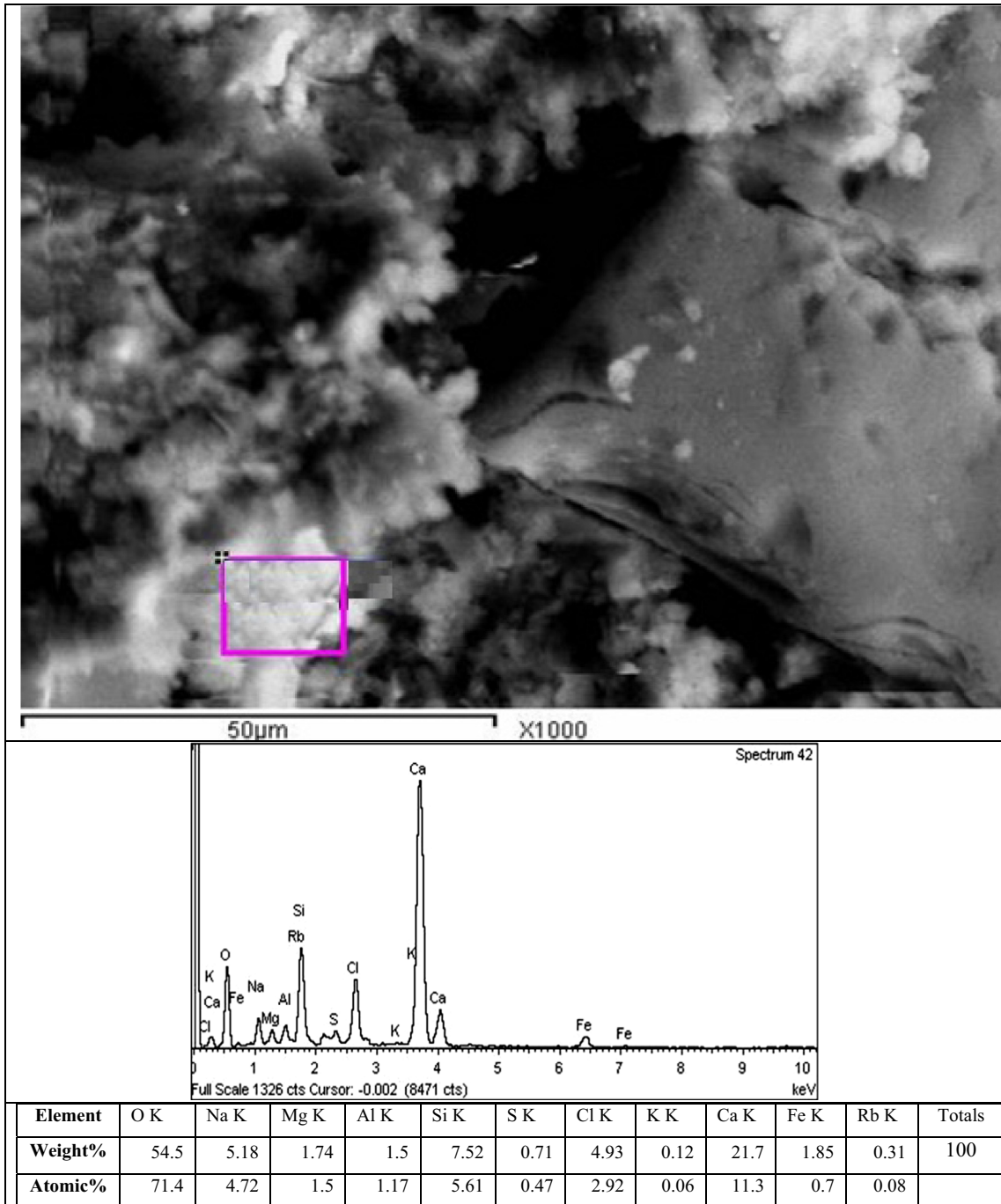| Element	O K	Na K	Mg K	Al K	Si K	S K	Cl K	K K	Ca K	Fe K	Rb K	Totals
Weight%	54.5	5.18	1.74	1.5	7.52	0.71	4.93	0.12	21.7	1.85	0.31	100
Atomic%	71.4	4.72	1.5	1.17	5.61	0.47	2.92	0.06	11.3	0.7	0.08	

Fig. 12. SEM and its corresponding EDX analysis for Q87 at depth 10 mm.

- The SEM images with corresponding EDX and mapping showing the places of these compounds and its constituting elements is accurately specified.

- Mapping is alternative method to conventional X-ray diffraction (XRD). Mapping can identify chemical elements in concrete sample.
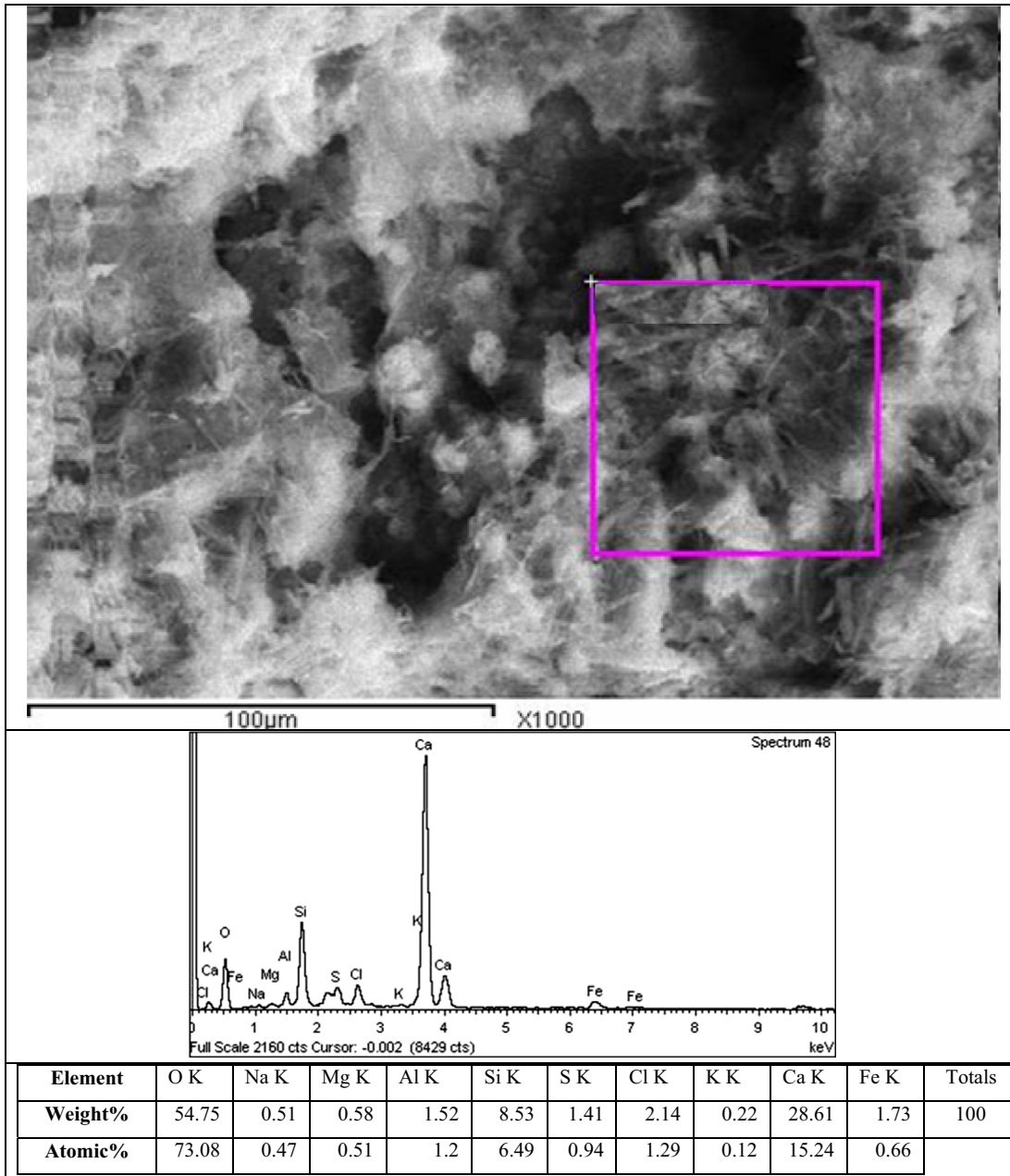
Element	O K	Na K	Mg K	Al K	Si K	S K	Cl K	K K	Ca K	Fe K	Totals
Weight%	54.75	0.51	0.58	1.52	8.53	1.41	2.14	0.22	28.61	1.73	100
Atomic%	73.08	0.47	0.51	1.2	6.49	0.94	1.29	0.12	15.24	0.66	

Fig. 13. SEM and its corresponding EDX analysis for T85 at depth 15 mm.

- Mapping Technique determines the locations of cracks, voids, and capillary pipes pores in the examined specimen.
- EDX analysis prove that siliceous aggregate particles act as inert material with no chloride ions or sulfate ions could penetrate the sand particles. The visual inspection confirms this fact that all eroded parts are in the mortar only and left the natural siliceous aggregates protruded out.
- Limestone natural wedges can be used as a barrier layer for preventing concrete from deleterious actions. Where, EDX
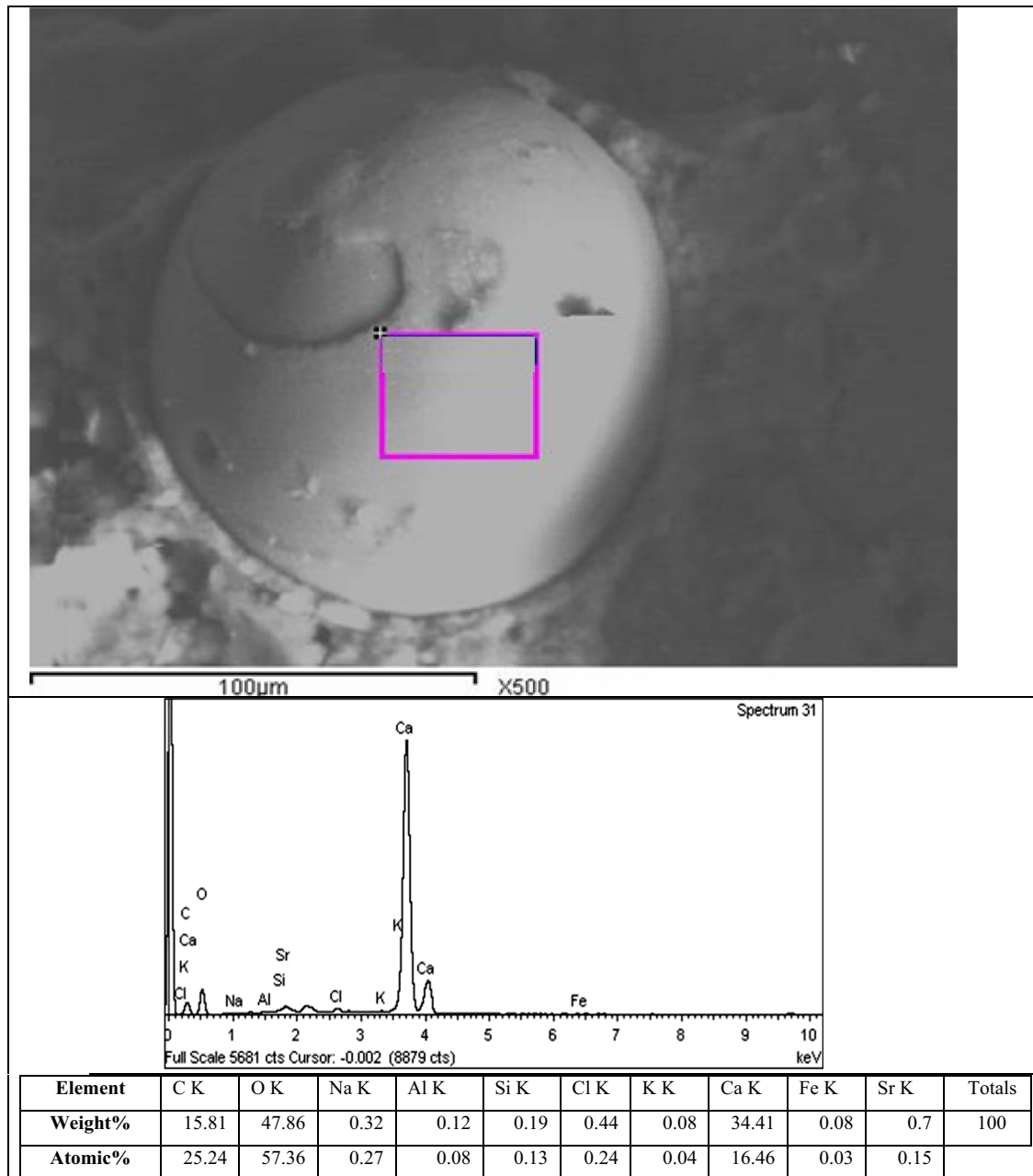
Element	C K	O K	Na K	Al K	Si K	Cl K	K K	Ca K	Fe K	Sr K	Totals
Weight%	15.81	47.86	0.32	0.12	0.19	0.44	0.08	34.41	0.08	0.7	100
Atomic%	25.24	57.36	0.27	0.08	0.13	0.24	0.04	16.46	0.03	0.15	

Fig. 14. SEM and its corresponding EDX analysis for Q50 at depth 80 mm.

analysis demonstrates that there are a few amounts of chloride ions can penetrate the limestone wedge but it is still more less than the amount of chloride ions at the surrounding cement paste.

• The non-preventative deterioration process of concretes subjected to seawater attack after long term period of exposure confirms the importance of using protective techniques.

Acknowledgements

References

[1] M.A.E. Aziz, S.A.E. Aleem, M. Heikal, H.E. Didamony, Hydration and durability of sulphate-resisting and slag cement blends in Caron's Lake water, Cem. Concr. Res. 35 (2005) 1592–1600.

[2] Manu Santhanam, Menashi Cohen, Jan Olek, Differentiating seawater and groundwater sulfate attack in Portland cement mortars, Cem. Concr. Res. 36 (2006) 2132–2137.

[3] Elke Gruyaert, Philip Van den Heede, Mathias Maes, Nele De Belie, Investigation of the influence of blast-furnace slag on the resistance of concrete against organic acid or sulphate attack by means of accelerated degradation tests, Cem. Concr. Res. 42 (2012) 173–185.

[4] Nader Ghafoori, Hamidou Diawara, Shane Beasley, Resistance to external sodium sulfate attack for early-opening-to-traffic Portland cement concrete, Cem. Concr. Compos. 30 (2008) 444–454.

[5] P.K. Mehta, Concrete in the Marine Environment, Elsevier Applied Science, London, 1991.

[6] A.M. Neville, Effects of freezing and thawing and of chlorides, in: Properties of Concrete, Longman, Essex, 1995.

[7] Ueli Angst, Bernhard Elsener, Claus K. Larsen, Øystein Vennesland, Critical chloride content in reinforced concrete — A review, Cem. Concr. Res. 39 (2009) 1122–1138.

[8] M.A.A. Al-khaled, Behavior of Concrete Containing Mineral Admixtures and Exposed to Aggressive Media (Ph.D thesis submitted to faculty of engineering), Cairo University, 2005.

[9] Hüseyin Yiğiter, Halit Yazıcı, Serdar Aydın, Effects of cement type, water/cement ratio and cement content on sea water resistance of concrete, Build. Environ. 42 (2007) 1770–1776.

[10] Tarek Uddin Mohammed, Hidenori Hamada, Toru Yamaji, Performance of seawater-mixed concrete in the tidal environment, Cem. Concr. Res. 34 (2004) 593–601.

[11] S.K. Kaushik, S. Islam, Suitability of sea water for mixing structural concrete exposed to a marine environment, Cem. Concr. Compos. 17 (1995) 177–185.

[12] O. Poupard, V. L'Hostis, S. Catinaud, I. Petre-Lazar, Corrosion damage diagnosis of a reinforced concrete beam after 40 years natural exposure in marine environment, Cem. Concr. Res. 36 (2006) 504–520.

[13] A. Leemann, R. Loser, Analysis of concrete in a vertical ventilation shaft exposed to sulfate-containing groundwater for 45 years, Cem. Concr. Compos. 33 (2011) 74–83.

[14] Nicoletta Marinoni, Marta Pellizon Birelli, Chiara Rostagno, Alessandro Pavese, The effects of atmospheric multipollutants on modern concrete, Atmos. Environ. 37 (2003) 4701–4712.

[15] Antonio Costa, Julio Appleton, Case studies of concrete deterioration in a marine environment in Portugal, Cem. Concr. Compos. 24 (2002) 169–179.

[16] Seashore Protection association (S.P.A) Alexandria directorate ElrasElsoda Alex.

[17] Cheng-Feng Chang, Jing-Wen Chen, The experimental investigation of concrete carbonation depth, Cem. Concr. Res. 36 (2006) 1760–1767.

[18] RILEM TC 178-TMC, Testing and modelling chloride penetration in concrete, Materials and Structures/Matériaux et Constructions, 2002, 35(November), 586–588.

[19] I. Monteiro, F.A. Branco, J. de Brito, R. Neves, Statistical analysis of the carbonation coefficient in open air concrete structures, Constr. Build. Mater. 29 (2012) 263–269.

[20] C. Andrade, J.M. Diez, C. Alonso, Mathematical modelling of a concrete surface skin effect on diffusion in chloride contaminated media, Adv. Cem. Mater. 6 (2) (1997) 36–44.

[21] G.R. Meira, C. Andrade, I.J. Padaratz, C. Alonso, J.C. Borba Jr., Chloride penetration into concrete structures in the marine atmosphere zone – Relationship between deposition of chlorides on the wet candle and chlorides accumulated into concrete, Cem. Concr. Compos. 29 (2007) 667–676.

[22] K.Y. Ann, J.H. Ahn, J.S. Ryou, The importance of chloride content at the concrete surface in assessing the time to corrosion of steel in concrete structures, Constr. Build. Mater. 23 (2009) 239–245.

[23] S. Sahu, S. Badger, N. Thaulow, R.J. Lee, Determination of water–cement ratio of hardened concrete by scanning electron microscopy, Cem. Concr. Compos. 26 (2004) 987–992.

[24] Paul E. Stutzman, Scanning Electron Microscopy in Concrete Petrography November 1–3, 2000, The American Ceramic Society, Anna Maria Island, Florida, 2001, pp. 59–72.

[25] N. Arreshvhina, Z. Fadhadli, H. MohdWarid, A.H. Zuhairy, Microstructural behavior of aerated concrete containing high volume of GGBFS, in: Proceedings of the 6th Asia-Pacific Structural Engineering and Construction Conference, (APSEC 2006) 5–6 September 2006, Kuala Lumpur, Malaysia, 2006.

[26] G.K. Glass, R. Yang, T. Dickhaus, N.R. Buenfeld, Backscattered electron imaging of the steel-concrete interface, Corros. Sci. 43 (2001) 605–610.

[27] M. Katsioti, N. Patsikas, P. Pipilikaki, N. Katsiotis, K. Mikedi, M. Chaniotakis, Delayed ettringite formation (DEF) in mortars of white cement, Constr. Build. Mater. 25 (2011) 900–905.

[28] Rui Luo, Yuebo Cai, Changyi Wang, Xiaoming Huang, Study of chloride binding and diffusion in GGBS concrete, Cem. Concr. Res. 33 (2003) 1–7.

[29] P.E. Grattan-Bellew, Microstructural investigation of deteriorated Portland cement concretes, Constr. Build. Mater. 10 (I) (1996) 3–16.

[30] M.T. Bassuoni, M.L. Nehdi, Durability of self-consolidating concrete to sulfate attack under combined cyclic environments and flexural loading, Cem. Concr. Res. 39 (2009) 206–226.